Deposition Rates of Silicon Carbide by Selected Area Laser Deposition

Y. L. Lee, J. V. Tompkins, J. M. Sanchez, and H. L. Marcus

Center for Materials Science and Engineering
The University of Texas at Austin

Abstract

The deposition rates using pure tetramethylsilane (TMS) as precursor are calculated numerically for a rod grown by the Selected Area Laser Deposition process. In particular, the dependence of the kinetics of deposition on pressure of TMS is examined. The conditions for which volcano deposition profiles occur are also investigated. The results show that deposition rate increases with increasing pressure and then becomes saturated. In addition, adsorption-desorption phenomena, rather than effects of reactants depletion, are responsible for the volcano deposition profile observed experimentally.

Introduction

Selected Area Laser Deposition (SALD) has seen rapid development during the past few years because of unique characteristics such as its local nature and its potential as a high deposition rate process. Therefore, laser chemical vapor deposition may be used to deposit a wide variety of materials for either prototypes or structural parts.

A considerable amount of work has been reported on the deposition of silicon carbide films because of their high mechanical and chemical performances: wear resistance and chemical stability [1]. However, few reports are available in which TMS is used as the precursor gas. Figueras et al. [2, 3, 4] reported several studies that use TMS for conventional CVD systems. They obtained the apparent activation energy, 90 kJ/mol, for the thermal decomposition of TMS using H_2 as a carrier gas. Sibieude and Benezech [5] also obtained the apparent activation energy for typical CVD systems using pure TMS precursor. They showed that the activation energy is function of pressure and substrate temperature. In 1994, Tompkins et al. [6] measured the deposition rate with varying TMS pressure for laser chemical vapor deposition.

Volcano-like profiles of deposition were often reported for laser chemical vapor deposition[7]. In general, these deposition profiles can be explained by several factors. They can occur when the reaction rate is much faster than the diffusion rate of the reactants[8]. In this case, the center of the spot is depleted of reactants relative to the periphery giving rise to the volcano-like deposition profile. The temperature dependence of the sticking coefficients also plays a role in the formation of the volcano profiles[9]. Finally, nonlinear kinetics model like Langmuir-Hinshelwood can also explain the volcano profiles [10].

The specific problem considered in this paper concerns the growth of a rod by a laser beam using pure TMS as gas precursor. Fig. 1 shows the geometry of the system. Deposition rates as well as temperature and TMS concentration profiles under different conditions are studied. In addition, the predicted deposition rates are compared with experimental results to check the validity of the model.

Mathematical and Numerical Model

Since in SALD the deposition occurs at a locally heated substrate, it is necessary to model first the temperature distribution in the substrate. Several analytical solutions with particular assumptions were obtained using Bessel transforms, Green's functions, or Fourier series expansion technique [11, 12, 13]. However, in this study numerical solutions are obtained by solving the heat conduction equations with variable properties. The governing equation for heat conduction is as follows:

$$\frac{\partial}{\partial x_i} k_e(T) \frac{\partial T}{\partial x_i} = \dot{q} \tag{1}$$

where $k_e(T)$ and $\dot{q}$ are the thermal conductivity and the heat source term, respectively. The effective thermal conductivity [14], $k_e(T) = k_s(1-\varepsilon)/(1+\phi k_s / k_g)$, is adopted because silicon carbide powder is used for a substrate to reduce the thermal conductivity. Here, k_s and k_g are the thermal conductivities for SiC solid and TMS gas, ε is the volume fraction of gas in the powder substrate, and ϕ is a constant which is about 0.034. The heat source term includes the heat from a laser beam and the heat loss by radiation. The effects of reaction heat and natural convection were assumed to be negligible in this study. A finite volume method was adopted to solve the conduction equations. The calculated temperature profile is then used as a boundary condition when the gas phase is analyzed.

The following transport equations, in which the effects of viscous dissipation and thermal diffusion (Soret effects) are neglected, are solved simultaneously for momentum, heat, and mass transfer:

continuity:
$$\frac{\partial}{\partial x_i}(\rho u_i) = 0 \tag{2}$$

momentum:
$$\frac{\partial}{\partial x_i}(\rho u_i u_j) = -\frac{\partial p}{\partial x_i} + g_i + \frac{\partial}{\partial x_i}\left(\mu\left(\frac{\partial u_i}{\partial x_j} + \frac{\partial u_i}{\partial x_j}\right) - \frac{2}{3}\mu \frac{\partial u_i}{\partial x_j}\delta_{ij}\right) \tag{3}$$

energy:
$$C_p \frac{\partial}{\partial x_i}(\rho u_i T) = \frac{\partial p}{\partial t} - \sum_k h_k \dot{w}_k + \frac{\partial}{\partial x_i}\left(k \frac{\partial T}{\partial x_i}\right) + \frac{\partial}{\partial x_i}\sum_k \left(h_k \rho D \frac{\partial m_k}{\partial x_i}\right) \tag{4}$$

species:
$$\frac{\partial}{\partial x_i}(\rho u_i m_k) = -\frac{\partial}{\partial x_i}\left(\rho D \frac{\partial m_k}{\partial x_i}\right) + \dot{w}_k \quad \text{for species k} \tag{5}$$

Here ρ, μ, D, C_p, and k are respectively the density, the viscosity, the diffusivity, the specific heat at constant pressure, and the thermal conductivity of the gas. Also, m_k is the mass fraction of species k, and $\dot{w}$ is the production rate per unit volume for the kth species. The explanation of other notations in the above equations can be found elsewhere[15].

In the above equations, several transport properties appear, which are function of temperature and pressure. Since experimental values of those properties are not available for TMS, the coefficients are derived from standard statistical mechanics theory[16]. The density is determined by the ideal gas law.

In addition, chemical reactions have to be taken into account. For most of chemical vapor deposition reactions, only rudimentary models concerning intermediate species are available and almost no kinetic data exist. Therefore, a single overall reaction is used in this

study, which utilizes empirical parameters fitted to measured deposition rate data. Pyrolysis of TMS has been investigated by Figueras et al. [4] in the growth of silicon carbide films. TMS decomposes according to the following overall reaction:

$$Si(CH_3)_4(g) \rightarrow SiC(s) + 3CH_4(g) \tag{6}$$

The applied boundary conditions for the momentum equations are no-slip condition on the substrate and Neuman condition for the outer boundary. For the energy equations, the temperature profile in the substrate was obtained from the thermal conduction analysis. For the species equations, a surface reaction rate was used as a boundary condition at the substrate. That is, the flux of TMS is equal to the first order reaction rate.

$$-\rho D \frac{\partial m_{TMS}}{\partial r} = M_{TMS}(k_A C_{TMS})_{surface} \tag{7}$$

Here, D is the binary diffusion coefficient of TMS in CH_4, $k_A = k_o \exp(-E/RT)$ is the first order rate constant, and M_{TMS} is the molecular weight of TMS. The activation energy, E, for the thermal decomposition of TMS was obtained from the experiment of Sibieude et al. [5]. Also, the preexponential factor, k_o, in the Arrhenius equation was determined using the growth rate at 20 torr obtained by Tompkins et al. [6]. The preexponential constant needed to fit the experimental growth rate was 2.1×10^8 m/s.

The above conservation equations are discretized by employing a finite volume method with collocated grid. For computation of the pressure field, the SIMPLE algorithm is employed[17].

Results and Discussion

Fig. 2 shows the calculated properties of TMS using a hard sphere approximation to describe molecular interactions. In this model, all properties are function of only temperature, except the binary diffusion coefficient which is function of both temperature and pressure. The binary diffusion coefficient is inversely proportional to gas pressure. Fig. 3 shows the temperature profiles with radial distance for two different laser powers. The volume fraction of gas (ε) of the powder substrate was 0.2 and the diameter of a laser beam was 500 μm. The calculated temperature profiles were close to a Gaussian distribution, where the maximum temperature occurs at the center of the laser spot.

Fig. 4 shows the typical distribution of temperature for 20 torr in the gas phase. Since the isotherms are almost spherical, it is believed that the diffusion effects are dominant over the natural convection effects at this low pressure. The TMS concentration distribution is illustrated in Fig. 5. Again, it is clear that the diffusion effects prevail over the natural convection effects.

The variation of the growth rates with TMS pressure is shown in Fig. 6. The calculated rates are compared with the experimental data of Tompkins et al. [6]. As mentioned before, the experimental growth rate at 20 torr was fitted to calculate the preexponential factor. The predicted rates are in excellent agreement with their data up to 80 torr. However, the predicted growth rate becomes saturated over 80 torr while the experimental data starts to decrease. The saturation of the deposition rate may be explained using the fact that the deposition rates depend on both the concentration of TMS and the diffusivity: as the TMS pressure increases, the concentration of TMS increases, but the diffusivity decreases. Thus, it is seen that these two counteracting factors are responsible for the saturation of the deposition rate. It is believed that

the decrease in experimental growth rate is due to the contamination of the reactor window by a byproduct of the reaction during the experiments.

Fig. 7 shows the profiles of deposition rate for several different reaction rates. The preexponential constant was arbitrarily increased to see whether the volcano profiles occur. It is clear from Fig. 7 that the depletion of reactants due to high reaction rate indeed causes the volcano deposition profiles to form. However, we recalled that the preexponential constant needed to fit the experimental growth rate was 2.1×10^8 m/s, for which the volcano effects were not observed. Thus, the effects of reactants depletion do not seem responsible for the volcano profiles observed experimentally.

The effects of sticking coefficients on the deposition profiles are shown in Fig. 8. The sticking coefficients used in this study is assumed to be 1 if $T < T_L$ and 0 for $T > T_H$, varying linearly between the two temperatures. The deposition profiles in Fig. 8 are obtained for T_L=1400 K with varying T_H. The volcano profile starts to form if T_H is lower than 1700K. Furthermore, no deposition occurs near the center of a laser spot for T_H=1500 K. Thus, the temperature dependence of the sticking coefficients can also explain the volcano profiles. Since the profiles are strongly dependent upon the two critical temperatures, it will be crucial to use correct T_L and T_H for numerical modeling.

Conclusion

The deposition rate of TMS by Selective Area Laser Deposition has been successfully obtained with a single overall reaction. The present study leads to the following conclusions: (1) The effects of natural convection on deposition rate are negligible since the operating pressure are relatively low; (2) The deposition rate increases with increasing TMS pressure and saturates at high pressure; (3) The temperature dependence of the sticking coefficient or nonlinear kinetics model, rather than the depletion of reactants, seems to be the more likely cause for the volcano-like profiles observed experimentally.

Acknowledgments

This material is based in part upon work supported by the Texas Advanced Technology Program under Grant No. CSME-ATPD-157.

References

1. E. Fitzer and D. Hegen 1979, Angew. Chem. Int. Ed. Ergl., vol. 18, pp. 295.
2. A. Figueras, S. Garelik, and R. Rodroguez-Clemente 1991, " A morphological and Structural Study of SiC layers obtained by LPCVD using Tetramethylsilane", Journal of Crystal Growth, vol. 100, pp. 528.
3. A. Figueras, S. Garelik, j. Santiso, and R. Rodroguez-Clemente 1992, "Growth and Properties of CVD-SiC layers using Tetramethylsilane", Material Science and Engineering, B11, pp. 83.
4. A. Figueras, S. Garelik, j. Santiso, and R. Rodroguez-Clemente, B. Armas, C. Combescure, R. Berjoan, J. M. Saurel, and R. Caplain 1991, "Growth and Properties of CVD-SiC layers obtained by LPCVD using Tetramethylsilane", Journal of Materials Science, vol. 23, pp. 1632.
5. F. Sibieude and G. Benezech 1988. "Chemical Vapor Deposition of Silicon Carbide: an X-ray Diffraction Study", Journal of Materials Science, vol. 23, pp. 1632.
6. J. V. Tompkins, R. Laabi, B. R. Birmingham, H. L. Marcus 1994, "Advances in Selective Area Laser Deposition of Silicon Carbide", Proceedings of the Solid Freeform Fabrication Symposium, The University of Texas at Austin, Texas.

7. O. Conde, A. Kar, and J. Marjumder 1992, "Laser Chemical Vapor Deposition of Tin Dots: A comparison of theoretical and experimental results", Journal of Applied Physics, vol. 72, pp. 754.
8. Y. Zeiri, U. Atzmony, J. Bloch, and R. R. Lucchese 1991, Journal of Applied Physics, vol. 69, pp. 4110.
9. L. Konstantinov, R. Nowak, and P. Hess 1990, Applied Surface Science, vol. 46, pp. 102.
10. D. C. Skouby and K. F. Jensen 1987, "modeling of Energy and Mass Transport in Laser-Assisted CVD I: Surface Morphology", Proceedings of SPIE, vol. 797, pp. 140.
11. H. E. Cline and T. R. Anthony, 1983, Journal of Applied Physics, vol. 48, pp. 3895.
12. M. Lax 1977, "Temperature Rise induced by a Laser Beam", Journal of Applied Physics, vol. 48, pp. 3919.
13. M. K. El-Adawi and E. F. Elshehawey, Journal of Applied Physics, vol. 60, pp. 2250.
14. S. Yagi and D. Kunii 1957, AIChE Journal, vol. 3, pp. 373.
15. P. A. Libby and F. A. Williams 1980. "Turbulent Reacting Flows", Springer-Verlag, New York, USA.
16. J. O. Hirschfelder, C. F. Curtiss, and R. B. Bird 1967. "Molecular Theory of Gases and Liquids", John Wiley and Sons Inc., New York, USA.
17. S. V. Patankar 1980, "A Numerical Heat Transfer and Fluid Flow", Hemisphere, New York.

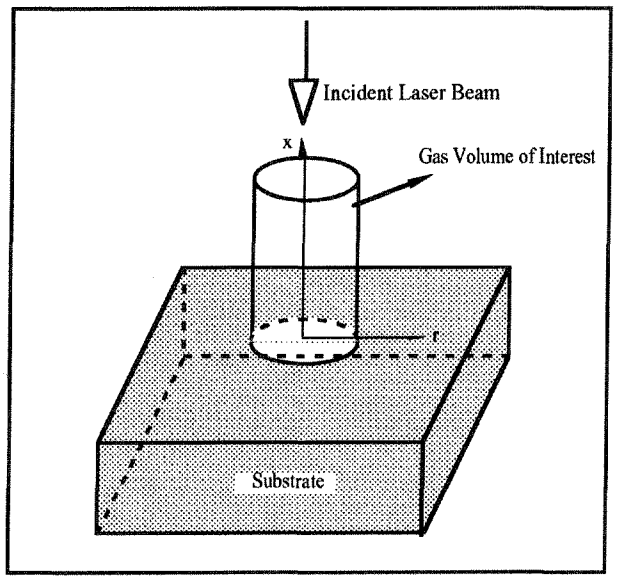

Fig. 1 Geometry of the system.

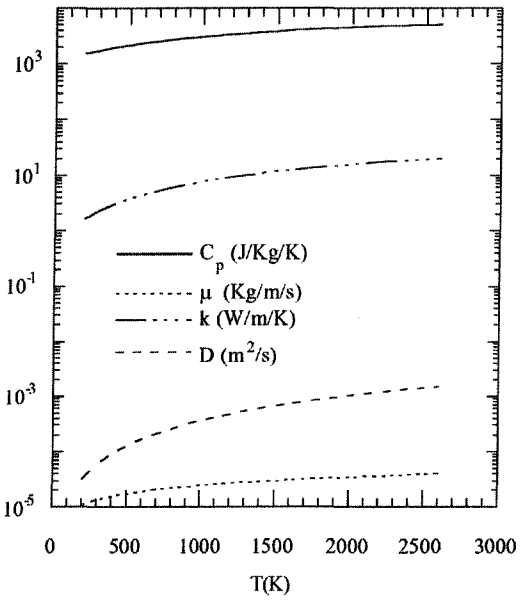

Fig. 2 Transport properties of TMS; D represents the binary diffusion coefficients of TMS in CH_4 at 20 torr.

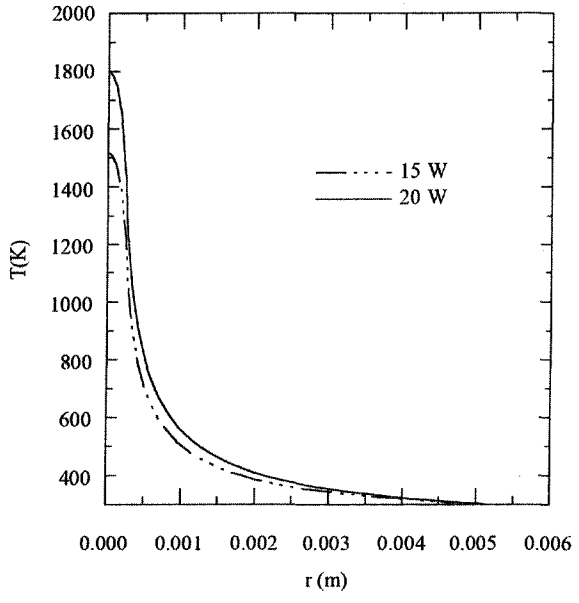

Fig. 3 Variation of temperature distribution with radial distance.

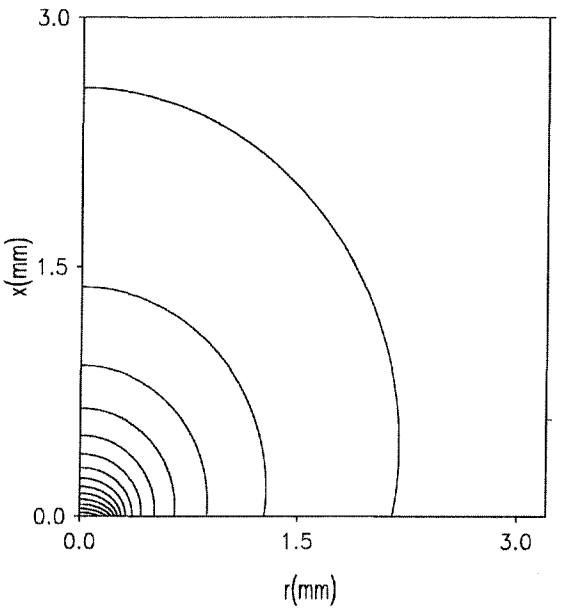

Fig. 4 Temperature distribution; from 1800 K to 400 K, step 100 K.

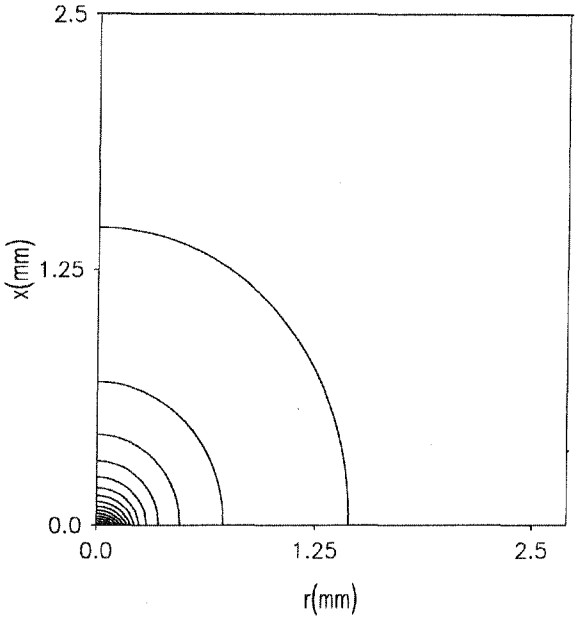

Fig. 5 Distribution of mass fraction of TMS; from 0.84 to 0.99, step 0.01.

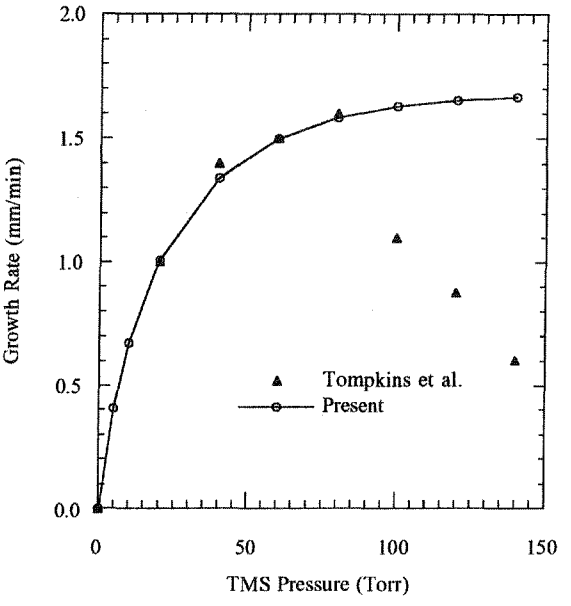

Fig. 6 Growth rate vs. TMS pressure

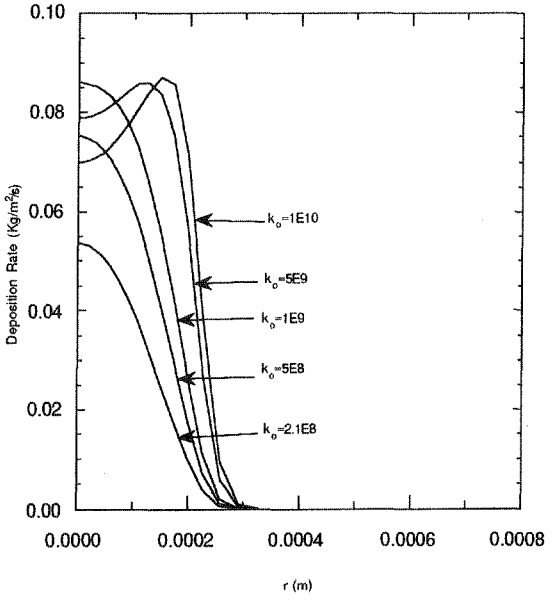

Fig. 7 Variation of deposition rate profiles with radial distance.

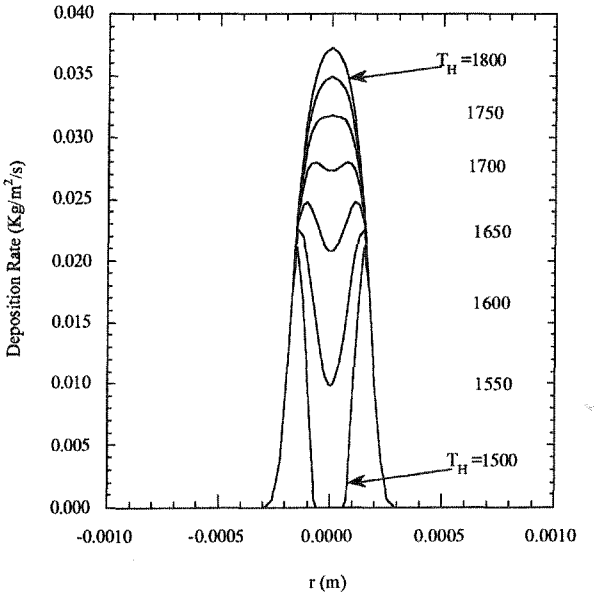

Fig. 8 Dependence of deposition rate profiles on sticking coefficients.